Chemical Product and Process Modeling

Volume 4, *Issue* 4 2009 *Article* 4

CHEMPOR 2008

Simulation of Membrane Separations Using a Modified Maxwell-Stefan Model

Paulo Brito, *Bragança Polytechnic Institute*
Licínio M. Gando-Ferreira, *University of Coimbra*
António Portugal, *University of Coimbra*

Recommended Citation:
Brito, Paulo; Gando-Ferreira, Licínio M.; and Portugal, António (2009) "Simulation of Membrane Separations Using a Modified Maxwell-Stefan Model," *Chemical Product and Process Modeling*: Vol. 4: Iss. 4, Article 4.
DOI: 10.2202/1934-2659.1314

Simulation of Membrane Separations Using a Modified Maxwell-Stefan Model

Paulo Brito, Licínio M. Gando-Ferreira, and António Portugal

Abstract

In this work, a modified Maxwell-Stefan model, which considers both the concentration polarization and the transport through the membrane, is tested for the simulation of Dextran T70 aqueous solutions filtration. Numerical simulations by solving the model equations with an adaptive resolution algorithm, based on the Adaptive Method of Lines, determined the concentration profiles in the polarization layer and inside the membrane pore. It is shown that the formation of significant solute accumulation at the membrane/polarization interface leads to high levels of apparent rejection. A tubular cross-flow ultrafiltration module, containing a tubular polysulfone membrane with a molecular weight cut-off of 50 kDa, was used to perform the experiments. The model is able to successfully simulate data in the high rejection/low flux region using an equilibrium constant K_{eq} of 0.25, but does not reproduce the observed rejection drop/ pressure build-up which occurs for increased fluxes, which may be due to limitations of the model itself.

KEYWORDS: modeling, ultrafiltration, Maxwell Stefan equation, apparent rejection, adaptive methods

Author Notes: Please send correspondence to Paulo Brito, tel: +351-273-303110, e-mail:paulo@ipb.pt.

INTRODUCTION

The modeling of mass transfer phenomena in solute separations through inert membranes is essential for the efficient design and optimization of these operations, namely ultrafiltration processes, widely applied in an important range of industries, that include food and biotechnological industrial processes.

There are many ways of analysing the mass transfer phenomena in ultrafiltration processes varying in their degree of complexity. The simplest models such the gel-polarization model, the resistance-in-series model, the osmotic pressure model, the Kedem-Katchalsky (KK) equations have been widely used to predict the permeate flux (Wijmans et al., 1985, Kozinski and Lightfoot, 1972, Kedem and Katchalsky, 1958¸ Suchanek, 2006). For a rigorous description of the transport of the solute through the membrane enabling the prediction of its rejection, two general approaches can be followed: the classical continuum descriptions and the hydrodynamic models. It has been demonstrated elsewhere that all the descriptions are special cases of the generalized Maxwell-Stefan (MS) equations derived from either statistical-mechanics, either from theory of irreversible thermodynamics (Deen, 1987, Noordman and Wesselingh, 2002). The Maxwell-Stefan approach is particulary suited for the description of multi-component mass transport because it provides a generic framework to handle multiple the friction forces between the species, including also the friction of each species with the membrane. The system can be considered ideal or not, being necessary to calculate thermodynamic effects in the non-ideality case. The MS equations have been used by several authors to describe the transport in membranes (Oers et al., 1997, Bellara and Cui, 1998, Noordman and Wesselingh, 2002, Vasan et al., 2006). In this work, we followed an approach to simulate the ultrafiltration of macromolecular solutions, in which the binary friction model derived by Kerkhof (1996) for describing the intramembrane transport was used. This model is a modification of the Maxwell-Stefan-Lightfoot equation, and includes both interspecies (diffusive) and species-wall forces.

The ultrafiltration process simulation provides an analysis of the solute rejection phenomenon, which, in general, depends on the solution components properties (namely, their molecular sizes), the membrane characteristics and the process operating conditions. Therefore, through the intramolecular transport modelation, one can quantify the influence of each former conditions in the refered rejection phenomenon. The global model include, beside the contribution of the intramembrane transport, the contribution of the transport in the layer polarization and the respective equations are partial differential equations (PDE's) defined in two different spatial regions. The solution of the equations, in most studies reported in the literature, is achieved using numerical schemes that are not sufficiently robust and therefore, cause problems of convergence and stability of the numerical method. The numerical strategy used for solution of the equations is

based on the application of an adaptive method with grid refinement developed by Brito and Portugal (1998). This strategy provided promising results in the simulation of PEG-3400 aqueous solutions ultrafiltration (Brito et al., 2004, Ferreira et al., 2003). Now, the purpose is to test the simulation performance for ultrafiltration of more massive solutes, specifically dextranT70.

MATHEMATICAL MODEL

The model equations consider both the polarization layer and the transport through the membrane based on the binary friction model. Hence, for the polarization layer, we have:

$$\frac{\partial c}{\partial t} = -\frac{\partial N}{\partial z} \tag{1}$$

with the flux, N, defined as,

$$N = -\left(D + D_t\right)\frac{\partial c}{\partial z} + u_v c \tag{2}$$

where, $D = D_{12}\Gamma_c$, being D, the Fickian diffusion coefficient; D_t, the turbulent diffusivity; D_{12}, the Maxwell-Stefan diffusion coefficient; and Γ_c, the thermodynamic factor. The turbulent diffusivity is defined assuming an unitary turbulent Schmidt number ($\mathrm{Sc_t} = \nu_t / D_t$), and taking account the turbulent kinematic viscosity computed by the Vieth correlation (Brito et al., 2004):

$$\frac{\nu_t}{\nu} = \left(\frac{2}{9}\pi\sqrt{3}\right)^3 \left(\frac{f}{2}\right)^{3/2} \left(y^+\right)^3 \tag{3}$$

with the normalized distance from the membrane wall, y^+, calculated by,

$$y^+ = \frac{y\langle u_t \rangle \sqrt{f/2}}{\nu} \tag{4}$$

Being f, the Fanning friction factor, defined by the Blasius equation, $f = \left(0.3164/4\right)\mathrm{Re}^{-0.25}$, and u_t, the circulating fluid velocity.

For the intramembrane transport, on the other hand, the molar concentration temporal gradient is given by:

DOI: 10.2202/1934-2659.1314

$$\varepsilon \frac{\partial c'}{\partial t} = -\frac{1}{\tau}\frac{\partial N_m}{\partial z} \tag{5}$$

in which, τ is the tortuosity factor, and ε is the porosity. The intramembrane flux, N_m, is calculated by:

$$N_m = -\frac{\Gamma_c}{G}\frac{\partial c'}{\partial z} + u_v \frac{F}{G} c' \tag{6}$$

where, F and G are the convective and friction factors respectively, defined as in Kerkhof (1996) for a monosolute system, with the solute and the solvent represented by subscripts 1 and 2, respectively:

$$F = \left(\frac{1}{D_{12}} + \frac{c_t^{\,2}\overline{V}_1\overline{V}_2}{B_o}\kappa_2 \right)\frac{\tau}{\varepsilon} \tag{7}$$

$$G = \left(\frac{1}{D_{12}} + \frac{c_t}{B_o}\left(\phi_2\kappa_1\overline{V}_1 + \phi_1\kappa_2\overline{V}_2\right) \right)\frac{\tau}{\varepsilon} \tag{8}$$

where, c_t is the total molar concentration, $B_o=r_p^2/8$, is the permeability parameter, r_p, the cylindrical pore radius, and $\overline{V}_i$, ϕ_i and κ_i are the molar volume, the volume fraction and the viscosity fractional coefficient of component i, respectively. The thermodynamic factor Γ_c is given by (Kerkhof, 1996):

$$\Gamma_c = 1 + c\frac{\partial \ln \gamma}{\partial c} - \frac{c}{c_t}\left(1 - \overline{V}_1 \Big/ \overline{V}_t\right) \tag{9}$$

however, ideal conditions are assumed.

The model is completed by the definition of: boundary conditions, fixed bulk concentration at the polarization layer extreme, and equilibrium and flux equalization conditions at the membrane/polarization and membrane/permeate interfaces;

$$\begin{aligned} &z = -\delta \quad \Rightarrow \quad c = c_b \\ &z = 0 \quad \Rightarrow \quad c' = K_{eq}c \;;\; N = N_m \\ &z = L_m \quad \Rightarrow \quad c' = K_{eq}c_p \;;\; N = u_v c_p \end{aligned} \tag{10}$$

where c_b and c_p are the bulk and the permeate concentrations and K_{eq} is the equilibrium partition coefficient. The value of this parameter depends on

geometrical factors and specific interactions between the solute and pore wall. According to the exclusion theory and for spherical solutes in cylindrical pores, K_{eq} only depends on the ratio of the molecular radius and the pore radius, λ: $K_{eq} = (1 - \lambda)^2$.

As initial conditions, zero concentration profile start-up was considered:

$$t = 0 \quad \Rightarrow \quad c = c_b \quad (z = -\delta) \quad \wedge \quad c = c' = 0 \quad (z > -\delta) \tag{11}$$

The problem is discretized in the spatial direction and solved in the temporal dimension until a steady-state profile is reached, which implies a constant profile for the flux over all the spatial domain. Therefore, a simulated stationary permeate concentration, c_p, becames available, that can be used to calculate the apparent solute rejection, R_{app}:

$$R_{app} = 1 - c_p / c_b \tag{12}$$

The fluxes profiles allow the computation of the pressure drop due to the flow and the simulated total pressure drop,

$$\Delta P_{flow} = \frac{\tau}{\varepsilon} \frac{RT}{B_o} \int_0^{L_m} c_t \sum_{i=1}^{2} \kappa_i N_i \overline{V}_i dz \tag{13}$$

$$\Delta P_{total} = \Delta P_{flow} + \sigma \, \Delta\Pi \tag{14}$$

where $\Delta\Pi$ is the osmotic pressure drop through the membrane and σ, the osmotic reflection coefficient. The membrane resistence may be computed relating the flow pressure drop and the flux using pure water filtration experiments.

$$R_m = \frac{\Delta P_{flow}}{\eta_w u_v} \tag{15}$$

On the other hand,

$$R_m = \frac{L_m}{B_o} \frac{\tau}{\varepsilon} = \frac{8 L_m}{r_p^{\,2}} \frac{\tau}{\varepsilon} \tag{16}$$

which allows the estimation of relations between the structural properties of the membrane, namely of τ/ε, a critical model parameter.

DOI: 10.2202/1934-2659.1314

For the particular monosolute system under study (dextran-1 and water-2), the following relations are used in the computation of the specified properties (Oers, 1994):

$$D = 5.96\times10^{-11} + 2.12\times10^{-11}\tanh\left(0.0284\rho - 1.491\right) \tag{17}$$

$$\Pi = 37.0\rho + 0.752\rho^2 + 76.4\times10^{-4}\rho^3 \tag{18}$$

and

$$\kappa_1 = \kappa_2\left(1 + \frac{\eta_{sp}}{\phi_1}\right) \tag{19}$$

$$\kappa_2 = {\eta_w}\big/{c_t RT} \tag{20}$$

with,

$$\eta_{sp} = a\rho\exp\left(b\rho\right) \tag{21}$$

where, ρ represents the solution mass concentration.

NUMERICAL SOLUTION

The numerical solution of a normalized version of the partial differential-algebraic equation system, defined over a space-time coordinate system of variables, is accomplished with an adaptive resolution algorithm, based on the Adaptive Method of Lines, and presented by Brito and Portugal (1998). This method is used to solve simultaneously the two modules of the model (polarization layer and membrane, vd. Figure 1) over a one-dimensional discretized space direction, in the time direction until a steady state solute concentration profile is reached.

The polarization layer/membrane and membrane/permeate boundaries are both represented by two nodes located very close to one another. The solution is computed at those pairs of nodes by solving two algebraic equations: the equilibrium and the flux equalization conditions.

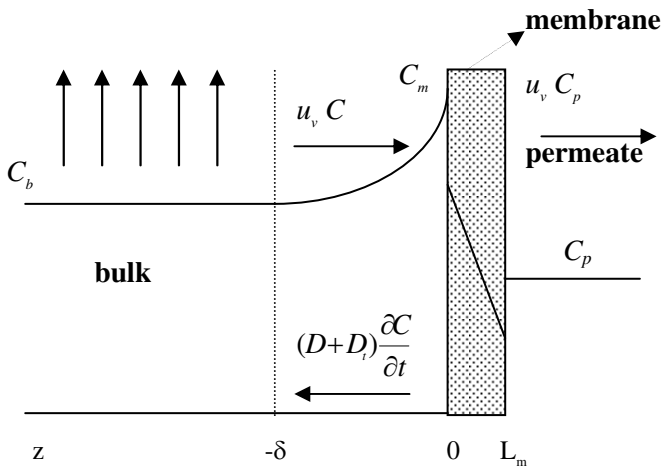

Figure 1. Simplified scheme representing the two spatial regions considered: polarization layer and membrane (membrane thickness is greatly exagerated for visualization purposes).

The spatial derivatives are approximated by central finite differences and the time integration is accomplished with DASSL numerical integrator. The normalized concentrations (y and y') are defined in relation to the bulk concentration, c_b, and the spatial coordinate ($-\delta \leq z \leq L_m$) is normalized to the total spatial domain extent:

$$z^* = \frac{z + \delta}{L_m + \delta} \tag{22}$$

being δ, the polarization layer size and L_m, the membrane thickness.

EXPERIMENTAL PROCEDURE

The experiments were performed in batch mode by using a tubular cross-flow ultrafiltration module containing a tubular polysulfone membrane of 1m and with a molecular weight cut-off of 50 kDa. The module has two separated permeate sections, being the samples for analysis collected from the section of the tube, where the entrance effects are absent. The procedure adopted consisted of varying the transmembrane pressure and to measure the permeation flux and the apparent rejection of Dextran T70 at two circulation velocities. The operating conditions, the solution components and membrane properties, and the simulation parameters used in the obtainance of all results presented in the next section, are summarized in Table 1.

DOI: 10.2202/1934-2659.1314

Table 1. Operating conditions, properties and simulation parameters.

Properties	Operational conditions and parameters
$\overline{V}_1 = 45.6$ m^3/kmol	$\rho_b = 10$ kg/m^3
$\overline{V}_2 = 0.018$ m^3/kmol	$u_t = 0.76$ m/s; 1.57 m/s Re = 1.2×10^4; 2.5×10^4
$L_m = 5\times10^{-7}$ m	$T = 298$ K
$r_p = 4.5\times10^{-9}$ m	$\delta = 86\times10^{-6}$ m
$\tau/\varepsilon = 26.018$	$MW = 98000$ Da

RESULTS AND DISCUSSION

A typical run provides evolutionary profiles like the ones presented in Figures 2 and 3, for normalized concentration (y and y') and space (z^*) variables.

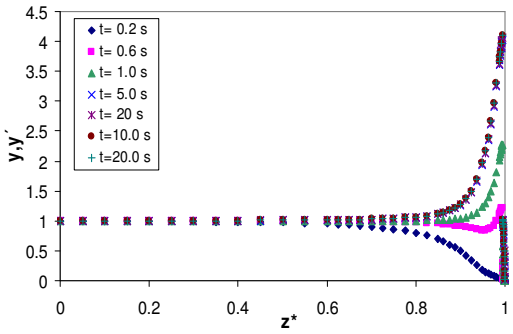

Figure 2. Normalized concentration profiles (polarization and membrane) in conditions: u_t= 1.57 m/s, u_v= 1.0×10^{-5} m/s and K_{eq}= 0.25.

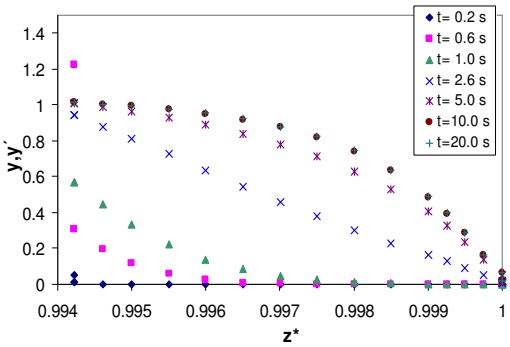

Figure 3. Normalized concentration profiles (membrane) in conditions: u_t= 1.57 m/s, u_v= 1.0×10^{-5} m/s and K_{eq}= 0.25.

The formation of significant solute accumulation at the membrane/polarization interface (in the presented case, the solute concentration is roughly four times higher than bulk concentration - c_b) and diminished permeate concentrations leading to high levels of apparent rejection of solute are verified.

The large levels of rejection are maintained over a reasonable range of flux values (vd. Figure 4). It is verified that fixing K_{eq} at 0.25 allows a good agreement between experimental and simulated results in the practically constant rejection area. However, it is observed a sudden important decrease in rejection beyond a flux threshold, which the model seems unable to replicate, in spite of a slight decreasing tendency that does not fit at all to the experimental data.

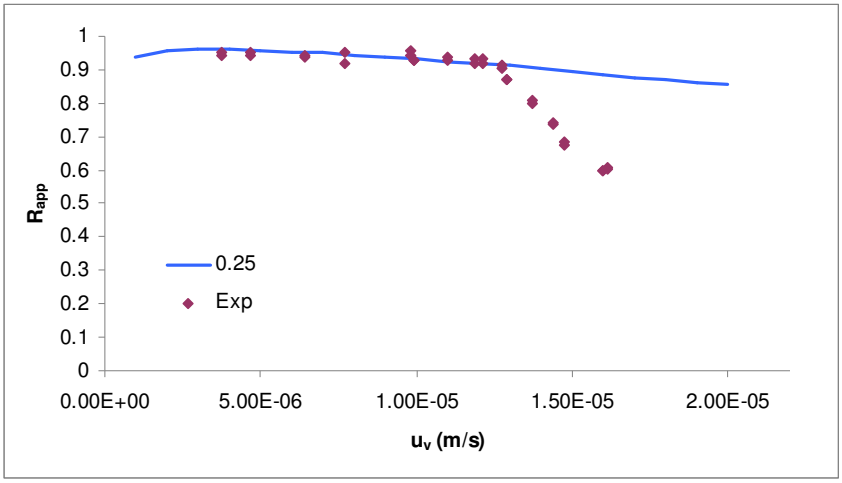

Figure 4. Apparent solute rejection profiles: u_t = 1.57 m/s, K_{eq} = 0.25.

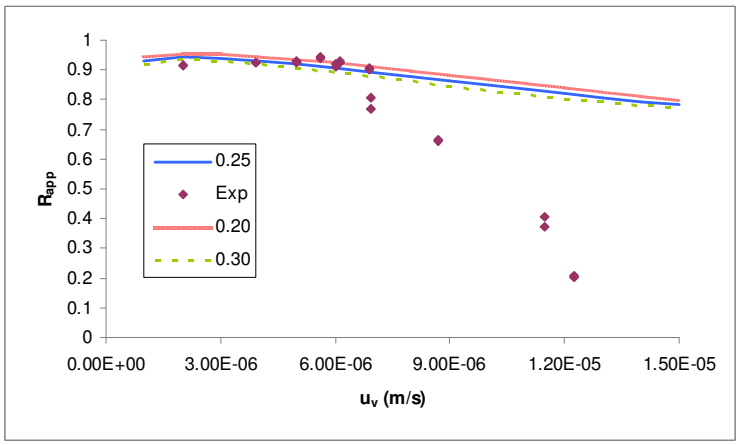

Figure 5. Apparent solute rejection profiles: u_t = 0.76 m/s, for various K_{eq}.

The problem stated above becomes more notorious for results concerning u_t = 0.76 m/s. In this case the decrease in rejection occurs earlier and in much stronger manner (vd. Figure 5). Again, the model can successfully replicate experimental results in the high plateau region with the same K_{eq} value, but fails to fit the sudden decrease.

These discrepancies may be due to two major reasons: phenomenon driven, main phenomena enter a different regime in which the model considerations become no longer valid; or parameter driven, the assumptions concerning parameter non-variance in the problem conditions are invalidated. Considering the later case, two important parameters able to affect considerably the results are: membrane resistance, R_m and equilibrium constant, K_{eq}. R_m is estimated using

DOI: 10.2202/1934-2659.1314

Pure Water Filtration (PWF) experiments in the same conditions (vd. Figure 6; in this case, $R_m = 5.1394\times10^{12}$ m^{-1}), a questionable procedure since it is noticeable a typical lack of reproducibility of this kind of PWF data due to compaction effects in the membrane. For PEG-3400 filtration experiments this procedure seems to be acceptable, because the experimental pressure drop profiles are very similar to the PWF ones (Brito et al, 2004). However this is clearly not the case in Dextran experiments. On the other hand, K_{eq} is assumed constant and it is the sole tuned parameter tuned to fit the experimental data available, as stated above. Therefore, it is chosen to test the sensitivity of the model toward these two parameters in order to explain the sudden rejection drop.

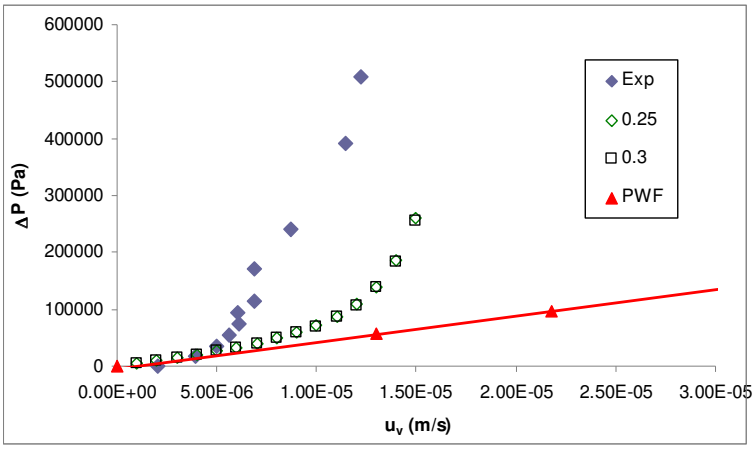

Figure 6. Total pressure drop profiles: u_t = 0.76 m/s, K_{eq} = 0.25; 0.30. (PWF- Pure Water Filtration)

It could be argued that this dramatic rejection drop would be due to sudden changes in the membrane geometry or structure. However, this behaviour suggests an important drop in membrane resistance R_m, which is inconsistent with the also dramatic increase in the pressure drop that occurs simultaneously with the rejection fall (vd. Figure 6). In general, this pressure drop rising should be connected with a resistance increase. The same conclusions could be driven by the analysis of the model behaviour to changes in K_{eq}. Changing these parameters values in the right direction to account the rejection evolution, will decrease its fitness of pressure data. Alternatively, the pressure drop rising conjugated with rejection drop could be explained with massive solute build-up at the membrane interface leading to extremely high solute concentration values (much higher than the computed by the model in these conditions – up to 30 times the bulk concentration). So, the pressure drop dramatic increase would be due essentially to the osmotic contribution.

The model provides a rise in pressure drop and the osmotic pressure drop contribution increases significantly for higher fluxes but overall this rise is insufficient to follow the experimental data. Similar conclusions could be drawn by the analysis of the u_t = 1.57 m/s experimental data, which are not presented here. Therefore, it is concluded that the behaviour observed is explained by phenomenogical features that are not successfully represented by the model used in the rejection drop zone, and that are particularly visible for lower values of u_t.

CONCLUSIONS

A coupled model of concentration polarization and membrane transport described by the binary friction model (BFM) is used to study the crossflow ultrafiltration of Dextran T70 solutions. A numerical procedure based on the adaptive method with grid refinement was able to give the solution of the system without much computational power and yield a rigorous solution of the problem.

It is concluded that the model successfully simulates experimental data in the high rejection/low flux region, but it is unable to replicate the observed rejection drop/pressure build-up which occurs for increased fluxes, which may be due to phenomenogical reasons or limitations of the model itself.

NOMENCLATURE

a, b – specific viscosity parameters [$m^3.kg^{-1}$];
B_o – permeability parameter [m^2];
c – molar concentration [$kmol.m^{-3}$];
D – *Fick* diffusion coefficient [$m^2.s^{-1}$];
D_t – turbulent diffusion coefficient [$m^2.s^{-1}$];
D_{12} – *Maxwell-Stefan* diffusion coefficient [$m^2.s^{-1}$];
f – *Fanning* friction coefficient [$kg.kmol^{-1}$];
F – convective factor [$s.m^{-2}$];
G – friction factor [$s.m^{-2}$];
K_{eq} – equilibrium partition constant [-];
L_m – membrane thickness [m];
MW – molecular mass [Da]
N – molar flux [$kmol.m^{-2}.s^{-1}$];
P – pressure [Pa];
r_p – pore radius [m];
R – ideal gas constant [$J.kmol^{-1}.K^{-1}$];
Re – *Reynolds* number [-];
R_m – membrane resistance [m^{-1}];
Sc – *Schmidt* number [-];

DOI: 10.2202/1934-2659.1314

t – time [s];
T – temperature [K];
u_t – circulating velocity [m.s^{-1}];
u_v – filtrate average flux [m.s^{-1}];
$\overline{V}$ – molar volume [m^3.kmol^{-1}];
y, z – spatial coordinate [m];

GREEK CHARACTERS

Γ_c – thermodynamic factor [-];
Π – osmotic pressure [Pa];
γ – activity coefficient [-];
δ – polarization layer thickness [m];
ε – membrane porosity [-];
η – viscosity [Pa.s];
κ – viscosity fractional coefficient [s];
λ - ratio of the molecular radius and the pore radius [-];
ν – kinematic viscosity [m^2.s^{-1}];
ρ – mass concentration [kg.m^{-3}];
σ – osmotic reflection coefficient [-];
τ – tortuosity [-];
ϕ – volume fraction [-];

REFERENCES

Bellara, S. R., Cui, Z. (1998) A Maxwell-Stefan approach to modeling the cross-flow ultrafiltration of protein solutions in tubular membranes, *Chem. Eng. Science*, 53 (12), 2153-2166.

Brito, P., Ferreira, L.M., Portugal, A., Blox, M., Kerkhof, P. (2004) Modelização de separações por membrana através de métodos de refinamento de malha. *Proceedings of Congresso de Métodos Computacionais em Engenharia*, Lisboa, Portugal, 473 & CD-ROM.

Brito, P.M.P., Portugal, A.A.T.G. (1998) Application of adaptive methods based on finite difference discretizations in the simulation of a tubular reactor system, *Proceedings of ACOMEN'98 – Advanced Computational Methods in Engineering,* Ghent, Belgium, 697-704.

Deen, W.M. (1987) Hindered transport of large molecules in liquid-filled pores, *AIChE Journal*, 33, 1409-1425.

Ferreira, L.M., Brito, P., Portugal, A., Blox, M., Kerkhof, P. (2003) A simulation study on the transport phenomena in ultrafiltration, *Workshop on Modelling and Simulation in Chemical Engineering*, Coimbra, Portugal, 8 p.

Kedem O., Katchalsky A. (1958) Thermodynamic analysis of the permeability of biological membranes to non-electrolytes. *Biochim. Biophys. Acta*, 27, 229-246.

Kerkhof, P.J.A.M. (1996) A modified Maxwell-Stefan model for transport through inert membranes: the binary friction model, *Chemical Engineering Journal*, 64, 319-343.

Kozinski, A. A., Lightfoot, E.N. (1972) Protein ultrafiltration: a general example of boundary layer filtration. *AIChE Journal*, 18, 1030-1040.

Noordman, T.R, Wesselingh, J.A. (2002) Transport of large molecules through membranes with narrow pores: the Maxwell–Stefan description combined with hydrodynamic theory. *Journal of Membrane Science*, 210, 227-243.

Oers, C.W., Vorstman M.A.G., v.d. Hout, R., Kerkhof P.J.A.M. (1997) The influence of thermodynamics activity on the solute rejection in multicomponent systems, *Journal of Membrane Science*, 136 (1), 71-87.

Oers, C.W. (1994) Solute rejection in multicomponent systems during ultrafiltration, Ph.D. Thesis, Eindhoven University of Technology.

Suchanek, G. (2006) Mechanistic Equations for Membrane Transport of Multicomponent Solutions, *Gen. Physiol. Biophys.*, 25, 53-63.

Vasan, S.S., Field, R.W., Cui. Z. (2006) A Maxwell-Stefan-Gouy-Debye model of the concentration profile of a charged solute in the polarisation layer, *Desalination*, 192, 356-363.

Wijmans, J.G., Nakao, S., Van Den Berg, J.W.A., Troelstra, F.R., Smolders, C.A. (1985) Hydrodynamic resistance of concentration polarization boundary layers in ultra-filtration, *Journal of Membrane Science*, 22, 117-135.

DOI: 10.2202/1934-2659.1314